

# RSC Advances



This is an *Accepted Manuscript*, which has been through the Royal Society of Chemistry peer review process and has been accepted for publication.

*Accepted Manuscripts* are published online shortly after acceptance, before technical editing, formatting and proof reading. Using this free service, authors can make their results available to the community, in citable form, before we publish the edited article. This *Accepted Manuscript* will be replaced by the edited, formatted and paginated article as soon as this is available.

You can find more information about *Accepted Manuscripts* in the [Information for Authors](#).

Please note that technical editing may introduce minor changes to the text and/or graphics, which may alter content. The journal's standard [Terms & Conditions](#) and the [Ethical guidelines](#) still apply. In no event shall the Royal Society of Chemistry be held responsible for any errors or omissions in this *Accepted Manuscript* or any consequences arising from the use of any information it contains.



Journal Name

## ARTICLE

# Alumina stabilized graphene oxide wrapped SnO<sub>2</sub> hollow sphere LIB anode with improved lithium storage

Received 00th January 20xx,  
Accepted 00th January 20xx

DOI: 10.1039/x0xx00000x

www.rsc.org/

Xiang Liu,<sup>a</sup> Qian Sun,<sup>a</sup> Alan M. C. Ng,<sup>a,b</sup> A. B. Djurišić,<sup>\*a</sup> Maohai Xie,<sup>a</sup> Baohu Dai,<sup>c</sup> Jinyao Tang,<sup>c</sup> Charles Surya,<sup>d</sup> Changzhong Liao,<sup>e</sup> Kaimin Shih<sup>e</sup>

SnO<sub>2</sub> hollow spheres were stabilized by graphene oxide wrapping, by alumina coating deposited via atomic layer deposition (ALD), or the combination of the two methods and used in lithium ion battery anodes. We found that graphene oxide wrapping provides a better buffering of volume changes and results in reduced electrode pulverization and better preservation of the electrode morphology compared to bare SnO<sub>2</sub> hollow spheres. On the other hand, ALD coating provides a significant improvement in the rate performance of the anodes, and it could also improve the adhesion of the metal oxide to the conductive additive since the coating is applied to entire electrode. The combination of the two techniques results in anodes with superior cycling and rate performance, with specific capacity of 1176 mAh/g after 60 cycles at 0.1 A/g (compared to 115 mAh/g for bare hollow SnO<sub>2</sub> nanospheres) and specific capacity of 329 mAh/g at 2A/g charge/discharge rate (compared to 7 mAh/g for bare SnO<sub>2</sub> hollow spheres). The improvement in performance was attributed to the superior preservation of anode morphology after cycling.

## Introduction

Metal oxides, in particular metal oxide hollow structures,<sup>1</sup> and graphene<sup>2</sup> represent very promising materials for lithium ion battery (LIB) anode applications. Several metal oxides exhibit much higher theoretical specific capacity compared to the commonly used graphite anodes (372 mAh/g).<sup>1</sup> SnO<sub>2</sub> for example is an attractive candidate for an anode material due to its high theoretical capacity of ~780 mAh/g,<sup>3,5</sup> as well as low cost.<sup>5</sup> The biggest disadvantage of metal oxide materials is poor cycling performance and rapid capacity decrease due to large volume changes upon lithium intercalation/deintercalation.<sup>1</sup> Hollow structures have an advantage of high surface area, low density and high loading capacity which makes them of interest for LIB applications.<sup>1</sup> More importantly, hollow interior allows for significant improvements in accommodating volume variations and easing strain, resulting in reduced electrode pulverization.<sup>1</sup>

Despite improved performance of hollow structures compared to solid metal oxides, further improvements in the performance are needed for practical applications.

Consequently, various strategies have been employed to date to prepare SnO<sub>2</sub> (and semiconductor or metal oxide in general) based LIB anodes,<sup>3-24</sup> for example morphology optimization of the SnO<sub>2</sub>.<sup>3-6,9,14</sup> The preparation of SnO<sub>2</sub>-carbon and metal oxide-carbon composites in general is another strategy for preparing materials for improved LIB anodes, as well as other applications.<sup>4,7,8,10-13,15-23</sup> Among different forms of carbon, graphene is a particularly interesting material<sup>25</sup> for a variety of applications, including those in lithium ion batteries.<sup>26-28</sup> Although graphene has exceptional properties, it is typically grown by chemical vapour deposition and it is considerably easier to produce chemically modified graphene (graphene oxide or reduced graphene oxide) in large quantities.<sup>27</sup> Consequently, these materials have been used in LIB electrodes.<sup>27</sup> It has been shown that graphene oxide encapsulation or wrapping is a particularly promising strategy,<sup>19,20,22</sup> and it yields improved performance compared to simple component mixing.<sup>19</sup> Furthermore, it has been shown that graphene wrapping can result in improvement in the reduction of particle aggregation and the accommodation of volume changes and thus improvements in the cycling performance.<sup>2</sup> In addition to preparing metal oxide composites with carbon, atomic layer deposition (ALD) can also be used to prepare LIB electrode (both anode and cathode) materials with improved performance by thin coating of another material, usually metal oxide.<sup>14,29-40</sup> ALD has an important advantage of

<sup>a</sup> Department of Physics, University of Hong Kong, Pokfulam Road, Hong Kong. \*E-mail: dalek@hku.hk

<sup>b</sup> Department of Physics, South University of Science and Technology of China, Shenzhen, China;

<sup>c</sup> Department of Chemistry, University of Hong Kong, Pokfulam Road, Hong Kong

<sup>d</sup> Department of Electronic and Information Engineering, Hong Kong Polytechnic University, Hung Hom, Kowloon, Hong Kong.

<sup>e</sup> Department of Civil Engineering, University of Hong Kong, Pokfulam Road, Hong Kong

Electronic Supplementary Information (ESI) available: TEM and SEM images, comparison of cycling performance with 1 nm and 3 nm ALD alumina coating. See DOI: 10.1039/x0xx00000x

producing uniform and conformal coating with a precisely controlled thickness.<sup>29</sup> Among different oxide materials used for stabilization of LIB electrodes, alumina is commonly employed.<sup>29-31,33-36,38</sup>

In this work, we compared the two common SnO<sub>2</sub> stabilization techniques, namely carbon composite (graphene oxide wrapping)<sup>19,20</sup> and atomic layer deposition of alumina layer,<sup>29</sup> as well as their combination. These two techniques have both been proposed to improve battery performance of metal oxide anodes, but direct comparisons of the improvements achieved by one of the two techniques or their combination have been scarce. Here we show that the two techniques have different effects on the cycling and rate performances, and their combination yields optimal performance. Since graphene oxide wrapping gives better preservation of SnO<sub>2</sub> morphology compared to ALD coating, while ALD coating can improve adhesion to conductive material in the anode, the combination of the two techniques results in significant improvement in the performance.

## Experimental

### Synthetic procedures

SnO<sub>2</sub> hollow nanospheres were synthesized by a previously reported template assisted method using carbon nanospheres as templates.<sup>16</sup> Briefly, 0.4g cetyltrimethyl ammonium bromide (CTAB) and 6.0g D-glucose were dissolved in 60 mL deionized water. After stirring for 30 min., the solution was transferred to a Teflon-lined autoclave and placed in an oven at 180°C for 10 h. Then the dark precipitates were washed by water and ethanol several times, collected and dried at 75°C. To prepare SnO<sub>2</sub> hollow spheres, the as-prepared carbon nanospheres (0.5 g) were then dispersed in 250 mL ethylene glycol by ultrasonication for about 2 h. Tin acetate (354.8 mg) was added in the solution and the solution was maintained at 120°C for 12 hours at oil bath on a hotplate. After the tin precursor loading, the samples were washed and dried again, and then annealed in air at 500°C for 4 hours (3°C/min ramping rate) to remove the carbon.

Graphene oxide nanosheet (GO) was synthesized from graphite (325 mesh) through a modified Hummers method.<sup>10</sup> Briefly, 180 mL concentrated H<sub>2</sub>SO<sub>4</sub> and 20 mL H<sub>3</sub>PO<sub>3</sub> were mixed in a beaker in an ice bath. At the same time, 1.5 g graphite powder and 9 g KMnO<sub>4</sub> were evenly mixed in a 500 mL round-bottomed flask. Then, the acid mixture was transferred into the flask slowly. Then the flask was placed into an oil bath at 50 °C and stirred overnight. After that, 200 mL cold water was added into the solution while stirring. Subsequently, H<sub>2</sub>O<sub>2</sub> was added into the solution drop by drop until the color of the solution became brilliant yellow. Then after stirring for another 3h, the mixture was washed with 0.05 M HCl (250 mL), de-ionized water and absolute ethanol respectively to remove unwanted ions. Finally, the graphene oxide nanosheets were collected and dried at 60 °C for 12h. Since GO nanosheets can be readily dispersed in water, they have been used directly for preparing GO wrapped hollow spheres. In addition to GO, reduced GO (rGO) can also be

considered as an anode material, but it requires additional synthesis steps (annealing or an addition of reducing agent during synthesis process, which adds to the process complexity and time needed for synthesis. Due to higher conductivity of rGO, it may represent a promising strategy for further improvements.

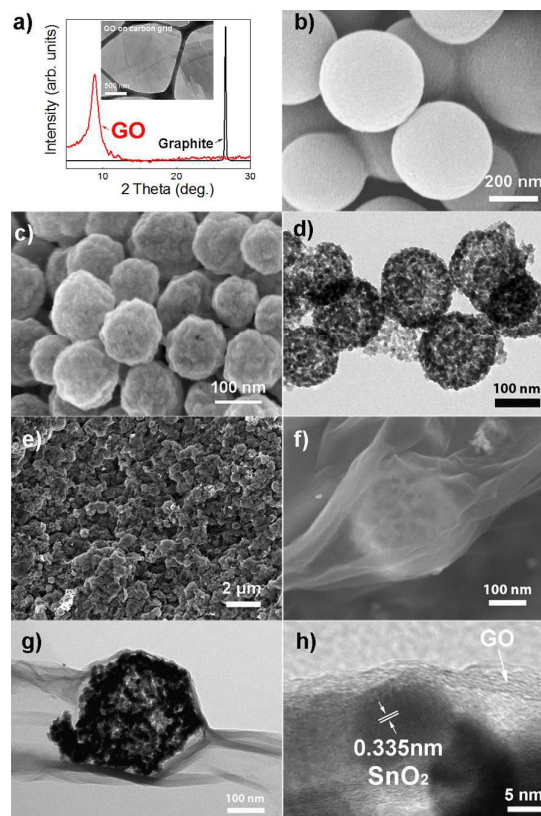


**Figure 1** (a) XRD patterns of graphite and reduced graphene oxide (inset is the typical TEM image of GO). (b) SEM image of synthesized carbon spheres. (c) SEM image of SnO<sub>2</sub> hollow spheres. (d) TEM image of SnO<sub>2</sub> hollow spheres. (e, f) SEM images of GO wrapped SnO<sub>2</sub> hollow spheres at different magnification. (g, h) TEM images of GO wrapped SnO<sub>2</sub> hollow sphere at different magnification.

The GO wrapped SnO<sub>2</sub> hollow spheres were synthesized by a modified previously reported method.<sup>17</sup> Typically, 0.1 g of as-prepared SnO<sub>2</sub> hollow spheres were dispersed into isopropanol (10 mL) by ultra-sonication for 5 min. Then 0.1 mL (3-aminopropyl)triethoxysilane (APTES) was added into the solution and the solution was mildly stirred for 24 h at room temperature. After that the products were washed with ethanol several times, and the APTES modified SnO<sub>2</sub> hollow sphere were dried and collected. To prepare GO wrapped SnO<sub>2</sub> hollow sphere, 0.1 g dried APTES modified SnO<sub>2</sub> hollow spheres were dispersed in 30 mL de-ionized water via ultra-sonication, and 20 mL of aqueous GO suspension (1 mg/mL) was added. After mildly stirring for another 3h, the GO wrapped SnO<sub>2</sub> hollow spheres were finally obtained.

$\text{Al}_2\text{O}_3$  ultrathin layer was coated directly on the prepared electrode by a Cambridge NanoTech Savannah 200 Atomic Layer Deposition System. It was previously shown that direct coating of the electrode results in better battery performance compared to the coating of the powder.<sup>34</sup> Trimethylaluminum (TMA) was used as aluminum precursor, while  $\text{H}_2\text{O}$  was used as the oxidizer. The deposition temperature was set at  $200^\circ\text{C}$ , and the growth rate was 0.11 nm per cycle. 10 and 30 cycles were used to get different thicknesses of coating layer.

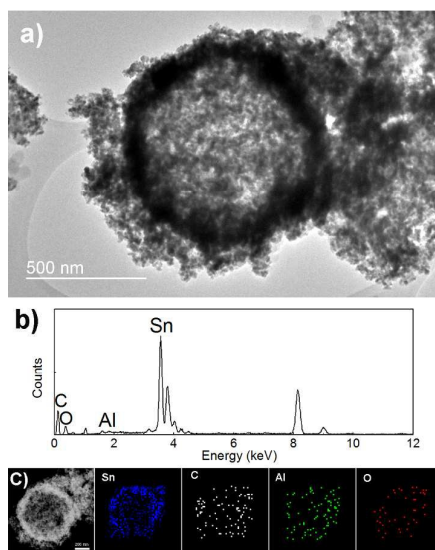


**Figure 2** (a) TEM image of  $\text{Al}_2\text{O}_3$  coated  $\text{SnO}_2$  HS/GO composite. (b, c) EDX spectrum and element mapping images of  $\text{Al}_2\text{O}_3$  coated  $\text{SnO}_2$  HS/GO composite.

The morphologies of electrodes before and after cycling were examined by scanning electron microscopy (SEM) using a Hitachi S4800 FEG System. Transmission electron microscopy (TEM) and energy dispersive X-ray (EDX) mapping were measured using a FEI Tecnai G2 20 S-TWIN and JEOL JEM-2011 Scanning Transmission Electron Microscope System. The active materials were mixed with the conductive carbon additives (carbon black, Super-P@Li, Timcal) and the binder (polyvinylidene fluoride, PVDF, MTI) in a weight ratio of 8:1:1. The loading amount of active material was about  $1 \text{ mg/cm}^2$ , and the specific capacity was calculated using an actual weight of the active material. Electrochemical measurements were conducted using a coin-cell (CR2032) with lithium metal as a counter-electrode. After coating and drying, electrodes were cut into 14 mm in diameter disks. Cells were assembled in Ar-filled glove box. The electrolyte consisting of 1 M  $\text{LiPF}_6$  in a 1:1:1 (in volume) mixture of ethylene carbonate (EC) /dimethyl carbonate (DMC) /diethyl carbonate (DEC) was purchased from MTI Corporation. Cyclic-voltammetry (CV) measurement was conducted at the rate of  $0.1 \text{ mV/s}$  in the range  $0.005 \sim 3.0 \text{ V}$  using a BioLogic VMP3 electrochemical workstation. The galvanostatic charge/discharge cycles were tested with a Neware BTS3000 battery test system at different current densities of  $100 \text{ mA}\cdot\text{g}^{-1} \sim 2 \text{ A}\cdot\text{g}^{-1}$  between 3.0 and 0.005 V. EIS measurements were performed using BioLogic VMP3

electrochemical workstation by employing an ac voltage of 5 mV amplitude in the frequency range of  $0.01 \sim 100 \text{ kHz}$ .

## Results and discussion

The samples in all steps of the synthesis were characterized in detail using electron microscopy and/or X-ray diffraction. Figure 1 shows the XRD patterns of graphite and reduced graphene oxide, as well as TEM image of graphene oxide. SEM images of carbon spheres, as well as SEM images of hollow  $\text{SnO}_2$  spheres (labeled  $\text{SnO}_2$  HS) are also shown. It is obvious that the spheres are hollow and consist of very small  $\text{SnO}_2$  nanoparticles. Successful graphene wrapping is obvious from both SEM and TEM images of graphene wrapped hollow spheres, labeled  $\text{SnO}_2$  HS/GO. Additional SEM and TEM images are shown in Supporting Information, Figures S1 and S2.

TEM image, EDX spectrum and element mapping of  $\text{SnO}_2$  HS/GO samples after ALD alumina coating are shown in Figure 2. It can be observed that aluminium is present in the samples, and that the element distribution is in agreement with the expectations from the sample composition.

Cycling performance and Coulombic efficiency of the samples are shown in Figures 3 and 4, respectively. For  $\text{SnO}_2$  hollow spheres, initial capacity of  $939 \text{ mAh/g}$  drops to  $571 \text{ mAh/g}$  by 2<sup>nd</sup> cycle,  $357 \text{ mAh/g}$  by 10<sup>th</sup> cycle, and  $115 \text{ mAh/g}$  at 60<sup>th</sup> cycle. From the obtained results, it is obvious that simple hollow morphology is insufficient to stabilize the electrode. Initial Coulombic efficiency of  $\text{SnO}_2$  HS samples of 44% increases to 95% by 24<sup>th</sup> cycle. With graphene oxide wrapping, we can observe improvements in the performance. Initial specific capacity is much higher,  $1447 \text{ mAh/g}$ , likely due to lithium storage contribution of GO. By 2<sup>nd</sup> cycle it drops to  $1059 \text{ mAh/g}$ , and by 20<sup>th</sup> cycle it still remains at  $1143 \text{ mAh/g}$  although by 60<sup>th</sup> cycle it drops to  $700 \text{ mAh/g}$ . Initial efficiency of 54% increases to 95% by 14<sup>th</sup> cycle.

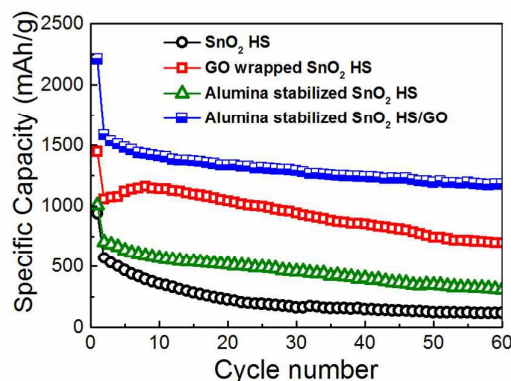


**Figure 3** Cycling performance of different electrodes at charge/discharge rate of  $100 \text{ mA/g}$ .

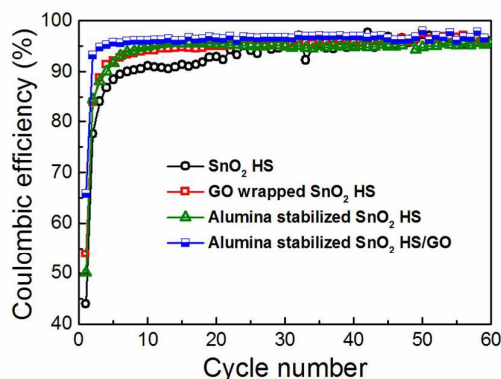


**Figure 4** Coulombic efficiency of different electrodes at charge/discharge rate of 100 mA/g.

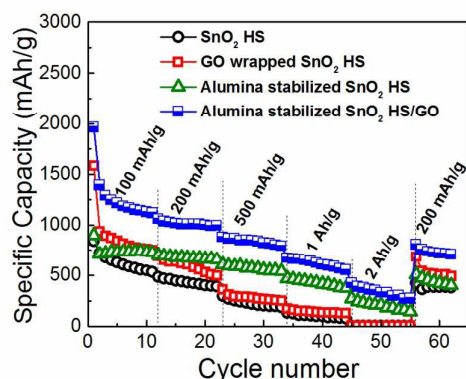


**Figure 5** Rate performance of different electrodes at charge/discharge rates from 100 mA/g to 2 A/g.

For alumina-coated  $\text{SnO}_2$  HS samples, initial capacity is similar to bare hollow spheres, 1008 mAh/g. By second cycle it drops to 707 mAh/g, and by 10<sup>th</sup> cycle it drops to 571 mAh/g. After 60 cycles, the specific capacity is 309 mAh/g, which is an obvious improvement over bare hollow spheres, but not as good as graphene wrapped hollow spheres. The initial efficiency of these samples was 50%, and it increased to 95% by 9<sup>th</sup> cycle. Finally, the samples with combined graphene wrapping and ALD coating exhibited the best performance with initial capacity of 2209 mAh/g (1582 mAh/g in the 2<sup>nd</sup> cycle) and the capacity of 1176 mAh/g after 60 cycles. The initial efficiency was 66%, and it rapidly increases to 96% by 5<sup>th</sup> cycle. It can be observed that the initial Coulombic efficiency of  $\text{SnO}_2$  is the lowest at 44%, while with GO wrapping and ALD coating it improves to 54% and 50% respectively. Both GO wrapping and ALD coating result in 66% initial Coulombic efficiency. This can likely be attributed to the improvement in the electrode stability (structural integrity)<sup>36</sup> and the reduction of the SEI formation. It was previously reported that ALD deposition of alumina coating directly on the electrode results in a stable artificial SEI layer.<sup>34</sup>

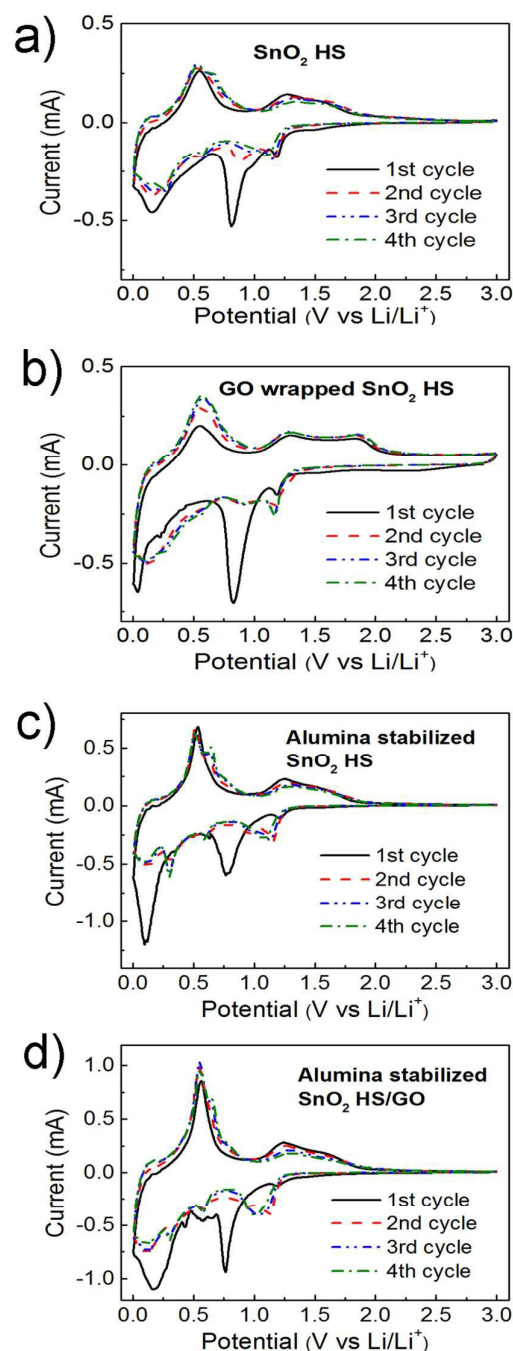


**Figure 6** The cyclic voltammetry curves of different  $\text{SnO}_2$  HS-based anodes (a)  $\text{SnO}_2$  HS, (b) GO wrapped  $\text{SnO}_2$  HS, (c) Alumina stabilized  $\text{SnO}_2$  HS, and (d) Alumina stabilized GO wrapped  $\text{SnO}_2$  HS at the first four cycles.

The rate performance of different anodes is illustrated in Figure 5. It can be observed that both  $\text{SnO}_2$  HS and  $\text{SnO}_2$  HS/GO samples exhibit inferior performance at high charge/discharge rates. For  $\text{SnO}_2$  HS we obtain 98 mAh/g at 1 A/g and 7 mAh/g at 2 A/g. Graphene oxide wrapping resulted only in a small improvement at high rates with 137 mAh/g at 1 A/g and

8 mAh/g at 2 A/g. On the other hand, alumina coating significantly improves the rate performance, with capacities of 417 mAh/g at 1 A/g and 211 mAh/g at 2 A/g. The rate performance is further improved with the employment of both GO wrapping and ALD coating, with specific capacities of 604 mAh/g at 1 A/g and 329 mAh/g at 2 A/g. It was reported that graphene wrapping of cobalt oxide hollow spheres improved both cycling and rate performance.<sup>41</sup> However, no rate performance improvement was obtained by simple mixing, although stable cycling performance was obtained.<sup>41</sup> It was also previously reported that ALD coating improved cycle life but reduced capacity at high rates, which was attributed to the fact that ALD layer served as a barrier to ion mobility.<sup>35</sup> In other works however, ALD coating resulted in improvements in both cycling and rate performance.<sup>32,36,40</sup> However, there was a difference in the effect of ALD coating in the rate performance of coated graphene and carbon nanotube samples.<sup>40</sup> Thus, it is likely that the morphology of the material and the thickness and properties of ALD coating would affect the overall electrochemical behavior.

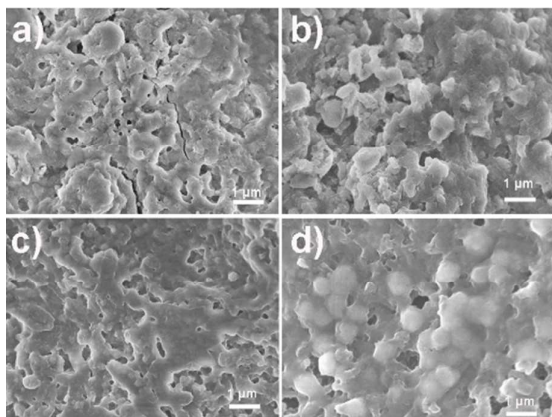
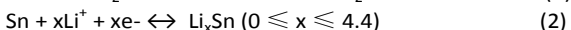
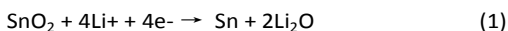


**Figure 7** SEM images of different SnO<sub>2</sub> HS-based electrodes after 60 cycles (a) SnO<sub>2</sub> HS, (b) GO wrapped SnO<sub>2</sub> HS, (c) Alumina stabilized SnO<sub>2</sub> HS, and (d) Alumina stabilized GO wrapped SnO<sub>2</sub> HS.

To obtain further insight into the mechanisms responsible for performance improvements for different electrode stabilization approaches, CV measurements were performed at the scan rate is 0.1 mV/s in the range between 5 mV to 3.0 V, as shown in Figure 6. Electrochemical storage mechanism of SnO<sub>2</sub> can be described as:<sup>5,6,10,22,24</sup>



In the first cathodic/anodic scans of all samples, several reduction/oxidation peaks can be resolved. The peaks in the range 0-0.6 V in the cathodic scan and the corresponding peaks in the region 0.4-0.9 V of the anodic scan can be attributed to Li-Sn alloying/dealloying processes.<sup>4-6,10,12,13,24</sup> Low voltage feature at ~0.01-0.1 V can also be partially due to Li intercalation into carbon.<sup>24</sup> For all samples, we can observe a significant peak at ~0.7-0.8V in the first cathodic scan, which

can be attributed to the irreversible reactions and the formation of the SEI layer.<sup>10,12,13</sup> This is in agreement with the significant capacity loss in the first cycle, which is commonly attributed to irreversible reactions and SEI formation.<sup>3,4</sup> The features at ~0.9-1.2 V in the cathodic scan and the corresponding feature at ~1.3 V in the anodic scan are due to partially reversible reduction of SnO<sub>2</sub> and oxidation of Sn, respectively.<sup>4-7,13</sup> For both GO wrapping and ALD alumina deposition, C-V curves in the second and subsequent cycles remain stable and exhibit the same shape, in agreement with literature reports on electrode stabilization by morphology optimization or ALD deposition.<sup>11,32,33</sup>

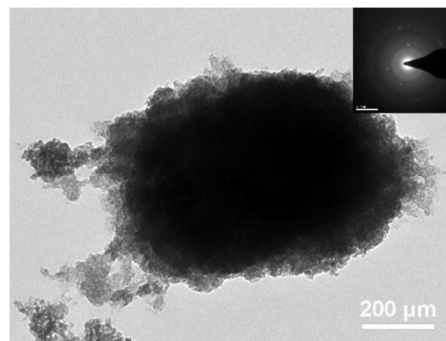


**Figure 8** A typical TEM image of alumina stabilized SnO<sub>2</sub> HS/GO electrode after 60 cycles (the inset is the relevant diffraction pattern of a single SnO<sub>2</sub> HS).

To further investigate the performance of different electrodes, we performed electron microscopy on the electrodes after cycling. Obtained SEM images are shown in Figure 7. We can observe that a better preservation of the original morphology is obtained after graphene wrapping, which is further improved by alumina stabilization. Mitigation of the mechanical degradation of the electrode by graphene nanosheet wrapping of hollow cobalt oxide spheres was identified as a significant contributor to the stable performance of such hybrid electrodes.<sup>41</sup> This is in agreement with the obtained results for cycling performance. It was reported that enclosing the metal oxide into an elastic and conductive carbon improves the performance by reinforcing the hollow structure and preventing aggregation.<sup>4</sup> While ALD coating is also expected to reduce electrode pulverization due to volume changes upon lithiation/delithiation,<sup>39</sup> very few intact spheres can be observed in samples with ALD coating only and without graphene wrapping. However, ALD coating was reported to create adhesion to the conductive additive, which would provide performance stabilization.<sup>39</sup> We also tried to deposit thicker alumina layers in an attempt to improve morphology stabilization by ALD coating. However, we found that significantly lower specific capacities are obtained for 3 nm (30 ALD cycles) coating of alumina compared to 1 nm (100 ALD cycles), as shown in Supporting Information, Fig. S3. In the case of SnO<sub>2</sub> HS/GO samples, while comparable performance is obtained for SnO<sub>2</sub> HS samples. This is likely due to the fact that too thick alumina layer can block lithium diffusion.<sup>30</sup> In

addition, alumina is an insulating material, and consequently there is an optimal thickness for good performance.

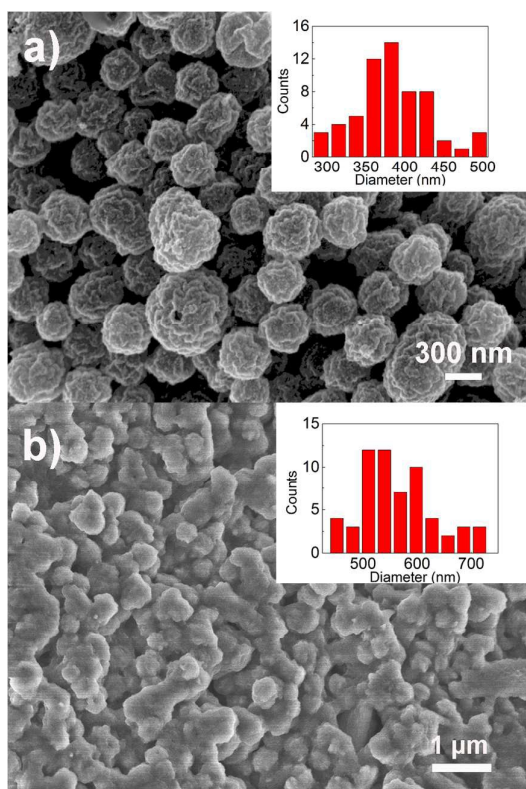


**Figure 9** SEM images of (a) as prepared SnO<sub>2</sub> HS (b) alumina stabilized SnO<sub>2</sub> HS/GO electrode after 60 cycles. The inset shows the sphere diameters.

To further investigate the effects of cycling on the morphology in alumina stabilized SnO<sub>2</sub> HS/GO samples, TEM imaging was performed. Obtained results are shown in Fig. 8, while additional TEM images can be seen in Supporting information, Figure S4. It can be observed that SnO<sub>2</sub> spheres after cycling no longer appear hollow. The size distribution of spheres is also changed, as illustrated in SEM images in Fig. 9. The change in the morphology from hollow porous spheres to dense spheres could possibly explain the initial irreversible capacity loss which would occur due to a significant reduction in the available surface area.

## Conclusions

Graphene oxide wrapping and ALD coating methods for stabilization of LIB electrodes consisting of SnO<sub>2</sub> hollow spheres are compared. Graphene oxide wrapping provides a better buffering of volume changes and results in reduced electrode pulverization and better preservation of the original electrode morphology. On the other hand, ALD coating provides a significant improvement in the rate performance of the anodes, and it could also improve the adhesion of the metal oxide to the conductive additive since the coating is

applied to entire electrode. Combination of the two stabilization techniques results in anodes with superior performance and a high degree of reversibility of the electrochemical reactions.

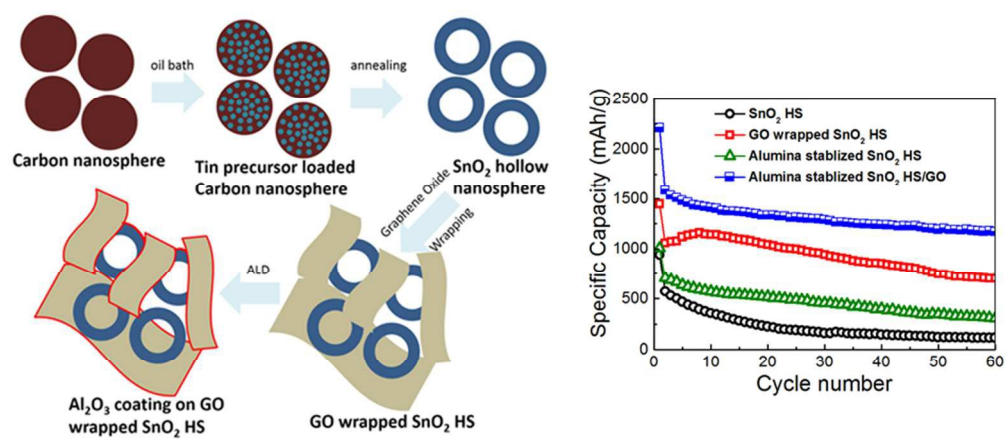
## Acknowledgements

Financial support from the Strategic Research Theme on Clean Energy and Seed Funding for Basic Research Grant of the University of Hong Kong is acknowledged. The authors would like to thank Prof. K. Y. Chan for the use of the electrochemical workstation.

## Notes and references

- 1 Z. Y. Wang, L. Zhou and X. W. Lou, *Adv. Mater.*, 2012, **24**, 1903.
- 2 F. Bonaccorso, L. Colombo, G. H. Yu, M. Stoller, V. Tozzini, A. C. Ferrari, R. S. Ruoff and V. Pellegrini, *Science*, 2015, **347**, 1246501-1.
- 3 V. Etacheri, G. A. Serisenbaeva, J. Caruthers, G. Daniel, J. M. Nedelec, V. G. Kessler and V. G. Pol, *Adv. Energy Mater.*, 2015, **5**, 1401289.
- 4 L. Zhang, H. B. Wu, B. Liu and X. W. Lou, *Energy Environ. Sci.*, 2014, **7**, 1013.
- 5 A. Bhaskar, M. Deepa and T. N. Rao, *Nanoscale*, 2014, **6**, 10762.
- 6 P. Gurunathan, P. M. Ette and K. Ramesha, *ACS Appl. Mater. Interfaces*, 2014, **6**, 16556.
- 7 J. Liang, X. Y. Yu, H. Zhou, H. B. Wu, S. J. Ding and X. W. Lou, *Angew. Chem. Int. Ed.*, 2014, **53**, 12803.
- 8 Z. Q. Zhu, S. W. Wang, J. Du, Q. Jin, T. R. Zhang, F. Y. Cheng and J. Chen, *Nano Lett.*, 2014, **14**, 153.
- 9 S. J. Han, B. Jang, T. Kim, S. M. Oh and T. Hyeon, *Adv. Funct. Mater.*, 2005, **15**, 1845.
- 10 Y. F. Dong, Z. B. Zhao, Z. Y. Wang, Y. Liu, X. Z. Wang and J. S. Qiu, *ACS Appl. Mater. Interfaces*, 2015, **7**, 2444.
- 11 Q. H. Tian, Z. X. Zhang, L. Yang and S. I. Hirano, *J. Power Sources*, 2015, **279**, 528.
- 12 Q. H. Tian, Y. Tian, Z. X. Zhang, L. Yang and S. Hirano, *J. Power Sources*, 2015, **280**, 397.
- 13 Y. Li, Q. Meng, J. Ma, C. L. Zhu, J. R. Cui, Z. X. Chen, Z. P. Guo, T. Zhang, S. M. Zhu and D. Zhang, *ACS Appl. Mater. Interfaces*, 2015, **7**, 11146.
- 14 C. Guan, X. H. Wang, Q. Zhang, Z. X. Fan, H. Zhang and H. J. Fan, *Nano Lett.*, 2014, **14**, 4852.
- 15 P. Wu, H. Wang, Y. W. Tang, Y. M. Zhou and T. H. Lu, *ACS Appl. Mater. Interfaces*, 2014, **6**, 3546.
- 16 J. Yue, X. Gu, L. Chen, N. Wang, X. L. Jiang, H. Y. Xu, J. Yang and Y. T. Qian, *J. Mater. Chem. A*, 2014, **2**, 17421.
- 17 D. H. Wei, J. w. Liang, Y. C. Zhu, Z. Q. Yuan, N. Li and Y. T. Qian, *Part. Part. Syst. Charact.*, 2013, **30**, 143.
- 18 J. S. Lee, K. H. You and C. B. Park, *Adv. Mater.*, 2012, **24**, 1084.

- 19 S. B. Yang, X. L. Feng, S. Ivanovici and K. Müllen, *Angew. Chem. Int. Ed.*, 2010, **49**, 8408.
- 20 Y. T. Xu, Y. Guo, C. Li, X. Y. Zhou, M. C. Tucker, X. Z. Fu, R. Sun and C. P. Wong, *Nano Energy*, 2015, **11**, 38.
- 21 M. Shahid, N. Yesibolati, M. C. Reuter, F. M. Ross and H. N. Alshareef, *J. Power Sources*, 2014, **263**, 239.
- 22 H. Yang, Z. H. Hou, N. B. Zhou, B. H. He, J. G. Cao and Y. F. Kuang, *Ceram. Int.*, 2014, **40**, 13903.
- 23 J. Zhu, G. H. Zhang, X. Z. Yu, Q. H. Li, B. G. Lu and Z. X. *Nano Energy*, 2014, **3**, 80.
- 24 X. Liu, F. Z. Liu, Q. Sun, A. M. C. Ng, A. B. Djurišić, M. H. Xie, C. Z. Liao, K. M. Shih, *ACS Appl. Mater. & Interfaces*, 2014, **6**, 13478.
- 25 A. K. Geim, *Science*, 2009, **324**, 1530.
- 26 R. J. Chen, T. Zhao, T. Tian, S. Cao, P. R. Coxon, K. Xi, D. Fairen-Jimenez, R. V. Kumar and A. K. Cheetham, *APL Mater.*, 2014, **2**, 124109.
- 27 J. Hassoun, F. Bonaccoro, M. Agostini, M. Angelucci, M. G. Betti, R. Cingolani, M. Gemmi, C. Mariani, S. Panero, V. Pellegrini and B. Scrosati, *Nano Lett.*, 2014, **14**, 4901.
- 28 E. Quesnel, F. Roux, F. Emieux, P. Faucherand, E. Kymaki, G. Volonakis, F. Giustino, B. Martin-Garcia and I. Moreels, S. A. Gursel et al., *2D Mater.*, 2015, **2**, 030204.
- 29 J. Liu and X. L. Sun, *Nanotechnology*, 2015, **26**, 024001.
- 30 Y. He, X. Q. Yu, Y. H. Wang, H. Li and X. J. Huang, *Adv. Mater.*, 2011, **23**, 4938.
- 31 M. P. Yu, A. J. Wang, Y. S. Wang, C. Li and G. Q. Shi, *Nanoscale*, 2014, **6**, 11419.
- 32 N. Yesibolati, M. Shahid, W. Chen, M. N. Hedhili, M. C. Reuter, F. M. Ross and H. N. Alshareef, *Small*, 2014, **10**, 2849.
- 33 D. N. Wang, J. L. Yang, J. Liu, X. F. Li, R. Y. Li, M. Cai, T. K. Sham and X. L. Sun, *J. Mater. Chem. A*, 2014, **2**, 2306.
- 34 Y. S. Jung, A. S. Cavanagh, L. A. Riley, S. H. Kang, A. C. Dillon, M. D. Groner, S. M. George and S. H. Lee, *Adv. Mater.*, 2010, **22**, 2172.
- 35 L. A. Riley, S. K. Atta, A. S. Cavanagh, Y. F. Yan, S. M. George, P. Liu, A. C. Dillon and S. H. Lee, *J. Power Sources*, 2011, **196**, 3317.
- 36 T. Hu, M. Xie, J. Zhong, H. T. Sun, X. Sun, S. Scott, S. M. George, C. S. Liu and J. Lian, *Carbon*, 2014, **76**, 141.
- 37 C. M. Ban, M. Xie, X. Sun, J. J. Travis, G. Wang, H. T. Sun, A. C. Dillon, J. Lian and S. M. George, *Nanotechnology*, 2013, **24**, 424002.
- 38 Y. S. Jung, P. Lu, A. S. Cavanagh, C. M. Ban, G. H. Kim, S. H. Lee, S. M. George, S. J. Harris, and A. C. Dillon, *Adv. Energy Mater.* 2013, **3**, 213.
- 39 L. A. Riley, A. S. Cavanagh, S. M. George, Y. S. Jung, Y. F. Yan, S. H. Lee, and A. C. Dillon, *Chem. Phys. Chem.* 2010, **11**, 2124.
- 40 X. Sun, M. Xie, J. J. Travis, G. K. Wang, H. T. Sun, J. Lian, and S. M. George, *J. Phys. Chem. C* 2013, **117**, 22497.
- 41 H. T. Sun, X. Sun, T. Hu, M. P. Yu, F. Y. Lu, and J. Lian, *J. Phys. Chem. C* 2014, **118**, 2263.



80x34mm (300 x 300 DPI)